Mineralogical Magazine (2023), **87**, 292–299
doi:10.1180/mgm.2023.4

CAMBRIDGE UNIVERSITY PRESS

Article

On the matildite–bohdanowiczite solid-solution series

Paul Alexandre* and Moses Aisida

Geology Department, Brandon University, 270 – 18th Street, Brandon, Manitoba, R7A 6A9, Canada

Abstract

A high-grade ore sample from the Cu–Zn–Au Photo Lake volcanogenic massive sulfide deposit (Flin Flon–Snow Lake greenstone belt, Manitoba, Canada) contains a Bi–Ag sulfo-selenide with a composition situated approximately in the middle of the S–Se substitution range (Se ≈ 0.86 apfu and S ≈ 1.05 apfu). These new data, combined with a literature compilation of all publicly available matildite and bohdanowiczite compositional data, reveal a nearly complete range of S–Se substitution between these two minerals, with only the section between $BiAgSe_{0.78}S_{1.18}$ and $BiAgSe_{0.25}S_{1.75}$ – about a quarter of the complete S–Se range – not yet documented. These observations suggest that a complete solid-solution series between matildite and bohdanowiczite, as previously suspected, might exist and in a manner similar to the galena–clausthalite complete solid-solution series.

Keywords: matildite, bohdanowiczite, solid solution, selenides, sulfides, mineral composition, bismuth, silver, isomorphic replacement

(Received 9 September 2022; accepted 16 January 2023; Accepted Manuscript published online: 25 January 2023; Associate Editor: David John Good)

Introduction

The minerals formed by the cations Bi, Pb and Ag and the anions S and Se are a large and complex group of sulfide, selenide and sulfo-selenide minerals, many of which are relatively rare. In addition to the pure end-members, such as galena, bismuthinite and acanthite (PbS, Bi_2S_3 and Ag_2S), and clausthalite, guanajuatite and naumannite (PbSe, Bi_2Se_3 and Ag_2Se), there are numerous approved mineral species combining these elements in varying proportions (Anthony *et al.*, 1990; Fig. 1). These are situated mostly between the Bi and Pb sulfide end-members, i.e. galenobismutite ($PbBi_2S_4$), cosalite ($Pb_2Bi_2S_5$) and lillianite ($Pb_3Bi_2S_6$), and the Bi and Ag sulfide end-members, i.e. pavonite ($AgBi_3S_5$), benjaminite ($Ag_3Bi_7S_{12}$) and matildite ($AgBiS_2$), among others (Anthony *et al.*, 1990). Examples of selenides with predominantly Se combining more than one of these cations are much fewer, with bohdanowiczite ($AgBiSe_2$) being one of the few representatives (Anthony *et al.*, 1990; Fig. 1).

There are also several species incorporating varying amounts of both S and Se, with the principal Bi, in examples such as nevskite (Bi(Se,S)), paraguanajuatite ($Bi_2(Se,S)_3$), laitakarite ($Bi_4(Se,S)_3$) and ikunolite ($Bi_4(S,Se)_3$), combining to occupy the full S–Se compositional continuum (e.g. Prsek and Peterec, 2008 and references within, Cook *et al.*, 2021). The galena–clausthalite continuum (PbS–PbSe) has been documented to represent a complete solid-solution series (e.g. Coleman, 1959; Förster, 2005). However, the acanthite–naumannite continuum, even though the full S_2Se_0–S_0Se_2 compositional range exists, is not a complete solid-solution series, as acanthite (monoclinic) and naumannite (orthorhombic) have different crystalline structures. Nonetheless a partial solid solution between these two Ag species has been suggested to exist at high temperatures, where both Ag_2S and Ag_2Se may exhibit a cubic crystalline structure (Kullerud *et al.*, 2018).

Examples of species containing both Bi and Pb and varying amounts of S and Se include wittite ($Pb_3Bi_4(S,Se)_9$), weibullite ($Pb_6Bi_8(S,Se)_{18}$), babkinite ($Pb_2Bi_2(S,Se)_3$) and mozgovaite ($PbBi_4(S,Se)_7$), among others (Anthony *et al.*, 1990).

There are also several sulfide (but not selenite) species incorporating the three cations in question for example: heyrovskýite ($Pb_4AgBi_3S_9$), gustavite ($PbAgBi_3S_6$), treasurite ($Ag_7Pb_6Bi_{15}S_{32}$) and vikingite ($Ag_5Pb_8Bi_{13}S_{30}$), among others (Anthony *et al.*, 1990).

The significant factor here is that the three main S–Se substitutions (PbS–PbSe, Bi_2S_3–Bi_2Se_3 and Ag_2S–Ag_2Se) have been documented for their full compositional range. However, the only possible Bi–Ag sulfide–selenide substitution (between matildite, $AgBiS_2$, and bohdanowiczite, $AgBiSe_2$) has not been reported for the entire S–Se substitution range. A possible complete matildite–bohdanowiczite solid solution has been invoked previously (Banas *et al.*, 1980; Sejkora and Skacha, 2015), however data to prove its existence are lacking. It is the purpose of this contribution to fill this lacuna by providing new data and compiling all available literature data for these two minerals.

The Photo Lake sample

The sample investigated originates from the high-grade ore of the Cu–Zn–Au Photo Lake volcanogenic massive sulfide (VMS) deposit in the Precambrian Flin Flon–Snow Lake greenstone

***Author for correspondence:** Paul Alexandre, Email: alexandrep@brandonu.ca
Cite this article: Alexandre P. and Aisida M. (2023) On the matildite–bohdanowiczite solid-solution series. *Mineralogical Magazine* **87**, 292–299. https://doi.org/10.1180/mgm.2023.4

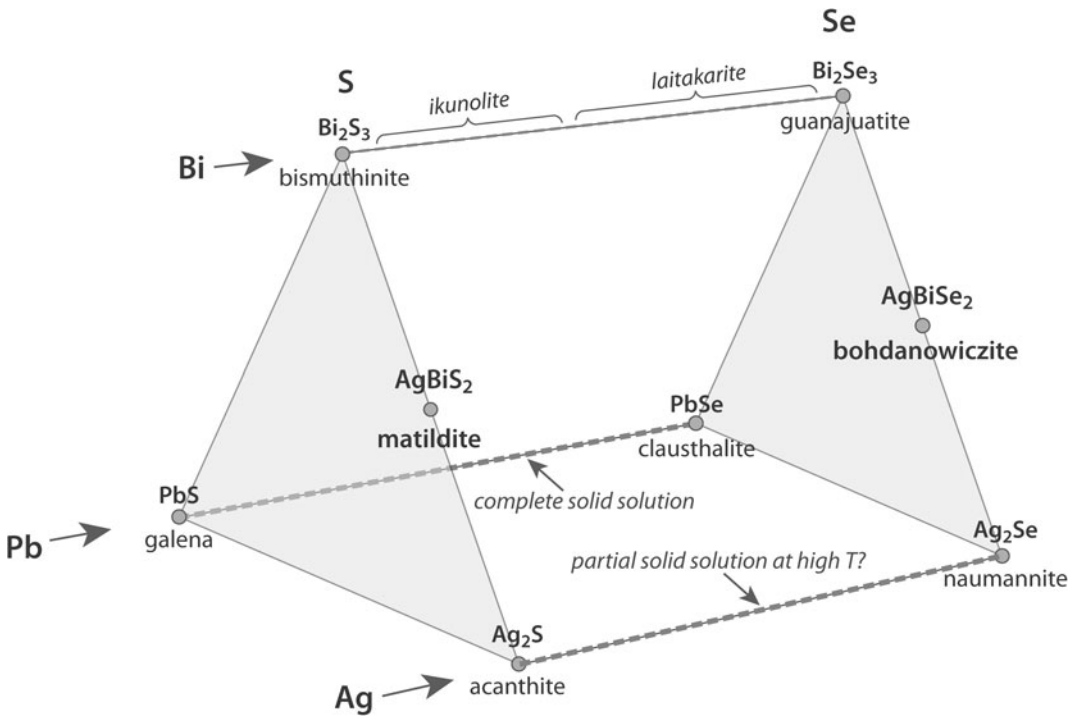

Fig. 1. The main Bi, Pb, and Ag sulfo-selenides, including end-members and intermediate mineral phases (Anthony *et al*., 1990). Several rare species are not included; the complete Pb solid solution and the possible Ag solid solution (at high temperature) are indicated (Coleman, 1959; Förster, 2005; Kullerud *et al*., 2018).

belt (Manitoba, Canada), which is a part of the Trans-Hudson orogeny and hosts several VMS deposits (e.g. Stern *et al*., 1995; Pehrsson *et al*., 2016; Alexandre *et al*., 2019). This deposit, discovered in 1994 and now mined out, contained 689,895 tons of ore at 4.58% Cu, 6.34% Zn, 0.60% Pb, 29.5 g/t Ag and 4.9 g/t Au (Pehrsson *et al*., 2016). It was hosted by the Photo Lake rhyodacite, a part of the mature arc section of the Snow Lake assemblage, and consisted of three massive, flattened, elongated and tightly folded lenses (Aisida, 2023 and references within).

The sulfide and ore mineralogy of the Photo Lake deposit is dominated by pyrite and economic amounts of chalcopyrite and sphalerite (Aisida, 2023). Pyrrhotite, arsenopyrite, galena and ilmenite are also present, in lesser amounts. A suite of accessory sulfide minerals present include gudmundite (FeSbS), gahnite ($ZnAl_2O_4$) and wurtzite ((Zn,Fe)S). Importantly, Bi species are also present (native bismuth and bismuthinite), together with some selenides such as clausthalite (PbSe), although in trace amounts (Aisida, 2023).

During an investigation on the ore mineralogy of several deposits in the Snow Lake area (Aisida, 2023) one mineral was identified tentatively as bohdanowiczite by semi-quantitative scanning electron microscopy (SEM) based on energy-dispersive spectrometry (EDS). During further investigation, as shown below, the composition was found to be situated approximately in the middle of the S–Se substitution continuum. Further characterisation of this member of the matildite–bohdanowiczite solid-solution family and evidence for the possible full solid-solution series is the main purpose of this investigation.

The matildite–bohdanowiczite mineral appears as very small (0.1 to 10 μm; predominantly <5 μm) anhedral to subhedral crystals (Fig. 2). These are predominantly found as inclusions in chalcopyrite and more rarely as individual crystals in the company of sulfide minerals. The matildite–bohdanowiczite inclusions in chalcopyrite are approximately aligned and seem to follow the chalcopyrite crystalline surfaces (Fig. 2b, c), which could be interpreted to indicate that they formed simultaneously (during the main ore stage at Photo Lake; Aisida, 2023), and that matildite–bohdanowiczite did not replace chalcopyrite later. However, it is worth noting that the textural relationship between matildite–bohdanowiczite and its chalcopyrite host (Fig. 2b, c) is reminiscent of chalcopyrite micro-inclusions within sphalerite ('chalcopyrite disease'), probably generated by the replacement of Fe-rich sphalerite by an aggregate of very fine-grained chalcopyrite within low-Fe sphalerite (Barton and Bethke, 1987). The mechanisms of this replacement might involve, among other processes, release of Bi at relatively high temperatures (Govindarao *et al*., 2018). It is possible to speculate that the relationship between chalcopyrite and the matildite–bohdanowiczite mineral was produced by similar processes, namely the exsolution of matildite–bohdanowiczite from a Bi- and Ag-rich chalcopyrite during partial melting due to the metamorphism that affected the deposit and its host rocks (Alexandre *et al*., 2019).

Analytical methods

Several thin sections were prepared from the sample and examined by optical microscopy (in reflected light) and by scanning electron microscopy at Brandon University, Canada using a JEOL JSM-6390 LV analytical SEM, equipped with an Oxford Instruments ULTIM MAX 100 Energy Dispersive Spectrometer characteristic X-ray detector and *Aztec 4.1* analytical software.

The composition of the matildite–bohdanowiczite was obtained by electron microprobe analysis using the Cameca SX-100 at the University of Manitoba. The operating conditions were: accelerating voltage 20 kV; current 10 nA and beam size 1 μm. The elements analysed were: Se (X-ray line used *Lα*,

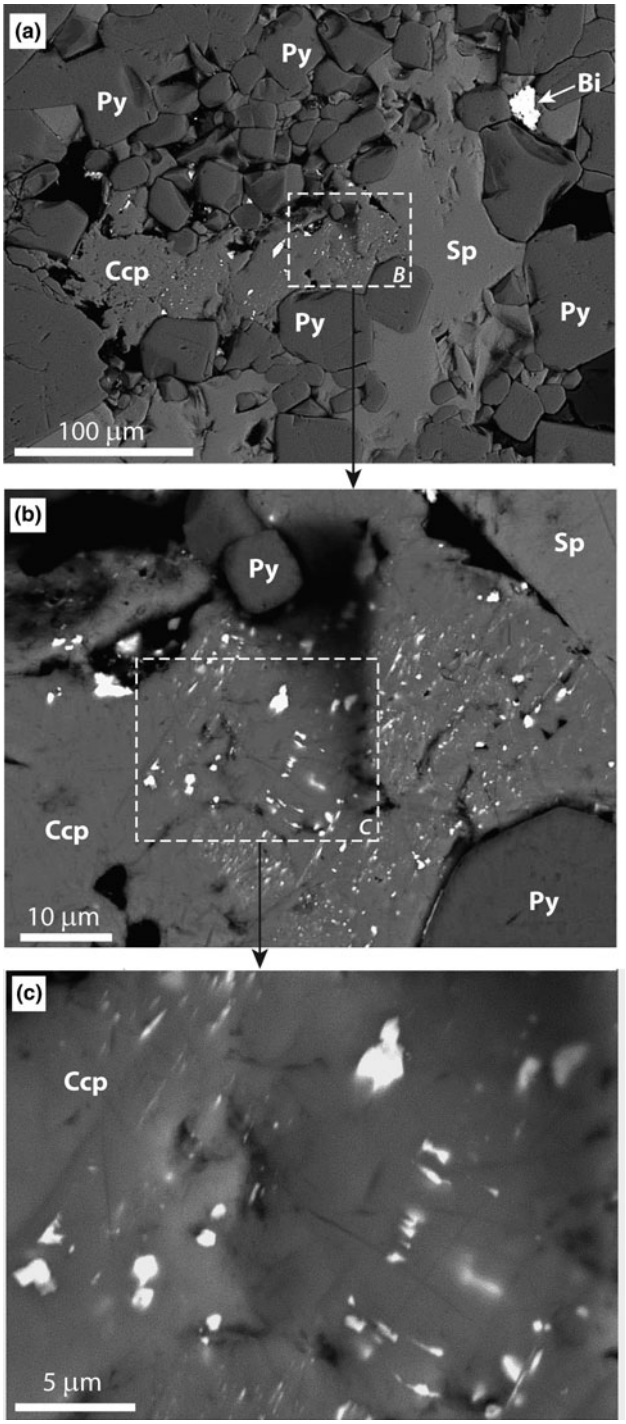

Fig. 2. Scanning electron microscope images of the matildite–bohdanowiczite mineral from the VMS Photo Lake deposit (Manitoba, Canada), seen here as inclusions within chalcopyrite (Ccp). Other minerals present are pyrite (Py), sphalerite (Sp) and native bismuth (Bi). No other minerals were identified in the chalcopyrite grain investigated here.

analytical crystal used TAP); Pb (*M*α, LPET); S (*K*α, LPET); Sb (*L*α, PET); Ag (*L*α, PET); Bi (*M*β, PET); Cu (*K*α, LLIF); Ni (*K*α, LLIF); Co (*K*α, LLIF); Fe (*K*α, LLIF); and Te (*L*α, LLIF). The peak counting times were 20 s with the exception of Se and S (30 s), with the background counted for half of that time, once on each side of the peak. The ZAF corrections followed the PAP procedure (Pouchou and Pichoir 1984; Pouchou and Pichoir 1985). Reference materials are natural and synthetic CdSe (for Se), PbTe (for Pb and Te), pyrite (for S and Fe), stibnite (for Sb), silver (for Ag), bismuthinite (for Bi), chalcopyrite (for Cu), pentlandite (for Ni) and cobalt (for Co).

Due to the very small grain size, typically smaller than the electron beam (Fig. 2c), several analytical spots excited the chalcopyrite host and were thus variably contaminated. Six analyses were rejected because of their unreasonably low totals. For the remaining analyses, the extent of the contamination was estimated based on the amounts of Bi and Se, both of which are absent in the chalcopyrite host (Aisida, 2023). Only data points showing no trace of contamination ($n = 4$) or with negligibly low amounts of contamination (well below 1 vol.%; $n = 3$) were retained, resulting in a relatively limited dataset of seven compositions. This low number necessarily affects the overall significance of this contribution, but it is worth noting that the few analyses reported here are truly representative of the matildite–bohdanowiczite solid-solution and can be considered with a high level of confidence. Statistical treatment of a few data points with low level of contamination (between 1 and 10 vol.%) was attempted in order to provide additional data, by estimating and subtracting the contamination. However, these re-calculated data are less reliable and inconsistent, and we considered it more prudent not to use them in this work.

Further data were compiled from all publicly available literature on the composition of bohdanowiczite and matildite, with the purpose of comparing their respective compositions to that of the mineral from the Photo Lake deposit (Canada). This compilation represents 17 sources (for 15 localities) for bohdanowiczite, from the first report describing the new mineral (Banas *et al.*, 1979) to the latest available paper (Cabral *et al.*, 2017). For matildite, eight sources have been compiled, ranging from the original description (reported in Palache *et al.*, 1944) to the latest available paper (Ivashchenko, 2021). The averages, minimum and maximum values for all literature data on bohdanowiczite and matildite, and for the matildite–bohdanowiczite solid-solution mineral from the Photo Lake deposit in Canada (this work) are reported in Table 1.

It was impossible to collect any structural data for the mid-series matildite–bohdanowiczite sample from the Photo Lake deposit, due to the excessively small grain size (Fig. 2c) and the very low amount of this mineral phase. If X-ray diffraction analysis had been performed on a bulk sample, the signal emanating from the small matildite–bohdanowiczite grain would be too low to be distinguished from the background noise. Further, micro-Raman is impossible to apply, not only because the smallest laser beam, 1 mm across, is larger than most of the matildite–bohdanowiczite solid-solution grains, but also because the method is not applicable to sulfide minerals, which oxidise under the laser beam and thus do not produce a recognisable spectrum or signature (Dr. A. Chakhmouradian, personal communication, Dec 1, 2022). In the absence of structural data, this work relies solely on the compositional characterisation of the sample to document the existence of the matildite–bohdanowiczite solid-solution series.

Results

Bohdanowiczite literature data

The literature data compilation for bohdanowiczite (Table 1) reveals average compositions of 44.74 wt.% Bi, 22.49 wt.% Ag and 29.90 wt.% Se. There are however some significant variations

Table 1. Average composition of bohdanowiczite and of matildite from literature data, obtained in most cases by electron microprobe analysis, and of the matildite–bohdanowiczite solid-solution mineral from Photo Lake, Canada (this work).

	All bohdanowiczite [1]			Photo Lake, Canada [2]			All matildite [3]		
Atomic	(*n* = 69)			(*n* = 7)			(*n* = 27)		
wt.%	min	mean	max	min	mean	max	min	mean	max
Bi	40.55	44.74	47.77	46.13	48.05	49.16	36.88	52.94	58.43
Ag	11.22	22.49	25.41	22.04	23.26	23.90	22.45	27.02	31.45
Pb	bdl	0.70	3.71		bdl		bdl	1.42	18.63
Cu	bdl	0.83	7.37	1.37	1.51	1.82	bdl	0.93	7.75
Fe	bdl	0.21	1.02	2.24	2.57	3.44		bdl	
Hg	bdl	0.15	0.45		bdl			bdl	
Co	0.01	0.02	0.02	bdl	0.01	0.02		bdl	
Ni	0.02	0.02	0.03		bdl			bdl	
Sb		bdl		0.17	0.34	0.47		bdl	
Se	20.21	29.90	34.60	15.48	17.14	19.20	bdl	0.92	4.94
S	bdl	1.86	5.73	7.47	8.38	9.63	14.29	16.29	17.53
Te	0.16	0.96	2.40	bdl	0.02	0.08		bdl	
Total	96.52	99.72	101.52	100.64	101.27	102.46	98.70	99.66	100.86
Atoms per formula unit, based on 4 ions									
Bi	0.910	0.991	1.040		0.925		0.700	0.967	1.100
Pb	bdl	0.018	0.085		bdl		0.000	0.026	0.350
Fe	bdl	0.018	0.053		0.182			bdl	
Hg	bdl	0.007	0.011		bdl			bdl	
Co	0.001	0.001	0.001		bdl			bdl	
Ni	0.002	0.002	0.002		bdl			bdl	
Sb		bdl			0.011			bdl	
Σ		1.036					1.118		0.993
Ag	0.470	**0.978**	1.080		**0.880**		0.750	**0.961**	1.073
Cu	bdl	**0.064**	0.525		**0.094**		0.000	**0.055**	0.440
Σ		1.042			0.974			1.016	
Se	1.129	**1.717**	2.060		**0.870**		0.000	**0.046**	0.246
S	0.005	**0.302**	0.788		**1.049**		1.753	**1.919**	2.020
Te	0.006	**0.030**	0.090		bdl			bdl	
Σ		2.049			1.919			1.965	

References: [1] sources for bohdanowiczite data are: Banas *et al.* (1979), Banas *et al.* (1980), Banas and Otterman (1967), Cabral *et al.* (2017), Belogub *et al.* (2020), Sejkora *et al.* (2017), Schonwandt (1983), Pringle and Thorpe (1980), Förster *et al.* (2005), Kovalenker and Plotinskaya (2005), Bondarenko *et al.* (2005), Kuznetsov *et al.* (2012), Sejkora and Skacha (2015), Cook and Ciobanu (2001), Thorpe *et al.* (1976), Pring (1988), Nesterov *et al.* (1985), and Zavyalov (1985); [2] this work; [3] sources for matildite data are: Vikentieva *et al.* (2008), Shizimu *et al.* (1998), Harris and Thorpe (1969), Palache *et al.* (1944), Lowry (1993), Triantafyllidis (2019), Satory *et al.* (2017), and Ivashchenko (2021).
bdl – below detection limit

between the different occurrences, with Bi varying between 40.55 and 47.77 wt.%, Ag between 11.22 and 25.41 wt.%, and Se between 20.21 and 34.60 wt.%.

The main substitution for Ag is Cu, as had been indicated previously (e.g. Förster *et al.*, 2005; Fig. 3), with the maximum individual analysis for Cu recorded at 7.37 wt.% at the Dognecea skarn deposits, SW Romania; the average Cu in bohdanowiczite from that deposit is 1.92 wt.% (Cook and Ciobanu, 2001). On average, bohdanowiczite contains 0.73 wt.% Cu.

Several elements can substitute for Bi in bohdanowiczite (Fig. 3), the main being Pb (0.70 wt.% on average, with a maximum of 3.71 wt.% recorded at the Roter Bär deposit, Germany: Cabral *et al.*, 2017); followed by Fe (an average of 0.21 wt.%, maximum of 1.02 wt.% at the Potashnya gold deposit, Ukraine; Bondarenko *et al.*, 2005), and Hg (0.15 wt.% on average, with a maximum of 0.45 wt.% at the Roter Bär deposit, Germany: Cabral *et al.*, 2017). Traces of Co and Ni, at levels barely above the detection limit, have also been documented (Table 1).

There are two possible substitutions for Se in bohdanowiczite: S (1.86 wt.% on average, with a maximum of 5.73 wt.% at the Moldava fluorite deposit, Czech Republic; Sejkora and Skacha 2015) and Te (an average of 0.96 wt.% with a maximum of 2.40 wt.% recorded at two deposits in Russia; Kovalenker and Plotinskaya 2005 and Kuznetsov *et al.*, 2012).

The overall empirical bohdanowiczite structural formula, based on the above averages and calculated for 4 ions, can be written as $(Bi_{0.961}Pb_{0.017}Fe_{0.017}Hg_{0.007})_{\Sigma 1.0003}(Ag_{0.948}Cu_{0.062})_{\Sigma 1.010}(Se_{1.665}S_{0.293}Te_{0.029})_{\Sigma 1.987}$.

Matildite literature data

The literature data compilation for matildite (Table 1) reveals average compositions of 52.94 wt.% Bi, 27.02 wt.% Ag and 16.29 wt.% S. Significant variations exist for these main constituents, with Bi varying from 36.88 to 58.43 wt.%, Ag from 22.45 to 31.45 wt.%, and S from 14.29 to 17.53 wt.% (Table 1).

The only cation substitutions recorded in matildite are Pb (1.42 wt.% on average, varying from undetectable to 18.63 wt.% in the Pitkäranta Mining District, Russia; Ivashchenko, 2021), Cu (0.93 wt.% on average, varying from below detection limit to 7.75 wt.% at the Berezovsk Gold Deposit in Russia; Vikentieva *et al.*, 2008), and minor Fe, with a single value of 1.65 wt.% reported in Greece (Triantafyllidis, 2019), but mostly below the detection limit (Table 1). Sulfur is substituted by Se (0.921 wt.% on average for a maximum of 4.94 wt.% at the Ikuno deposit in Japan; Shizimu *et al.*, 1998); Te has not been documented in matildite.

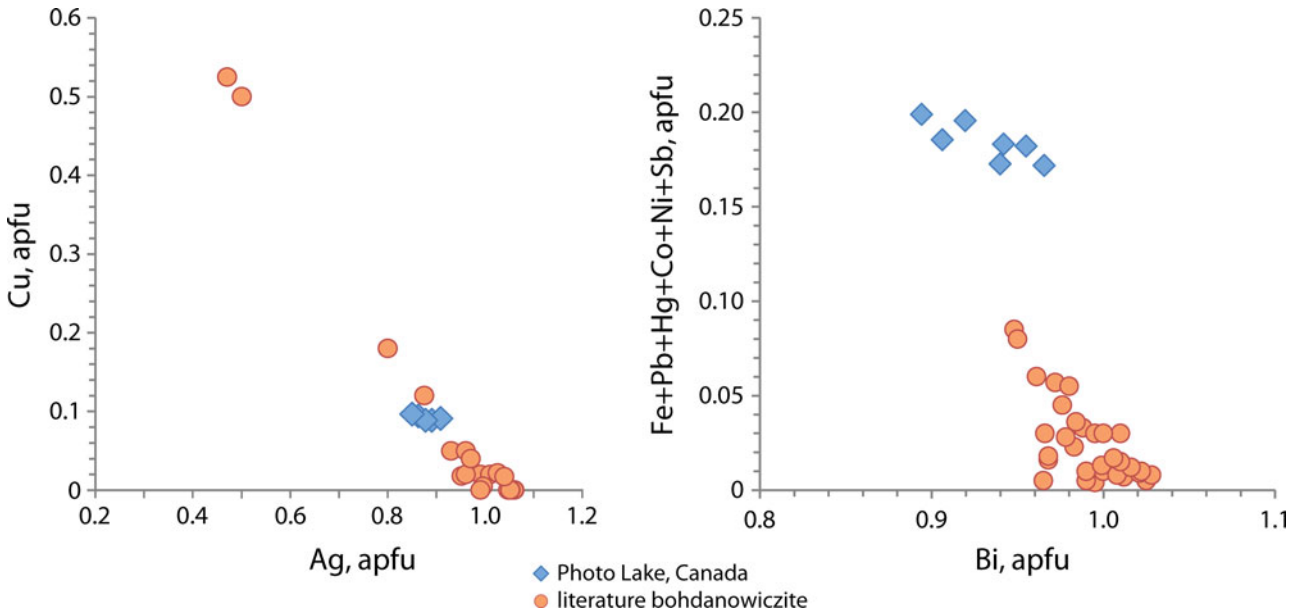

Fig. 3. Cationic substitutions in bohdanowiczite based on the literature data (Table 1) and this work. The only substitution for Ag is Cu (Cabral *et al.*, 2017), whereas a series of cations can replace Bi. The matildite–bohdanowiczite mineral from Photo Lake has greater Bi, Fe and Cu, the Fe clearly substituting for Bi.

The empirical structural formula for matildite, based on the above averages and calculated for 4 ions, can be written as $(Bi_{0.973}Pb_{0.026})_{\Sigma 0.993}(Ag_{0.967}Cu_{0.055})_{\Sigma 1.023}(S_{1.932}Se_{0.046})_{\Sigma 1.978}$ (Table 1).

The Photo Lake matildite–bohdanowiczite mineral

The matildite–bohdanowiczite sample described in this work from Photo Lake, Canada (Fig. 2) contains on average 48.05 wt.% Bi (from 46.13 to 49.16 wt.%), 23.26 wt.% Ag (from 22.04 to 23.90 wt.%), and 17.14 wt.% Se (from 15.48 to 19.20 wt.%; Table 1).

The main cation substitutions are Fe (an average of 2.57 wt.%), Cu (1.51 wt.%) and Sb (0.34 wt.%; Table 1). This is the only occurrence where Sb has been documented in bohdanowiczite or in matildite, considering all publicly available data (Table 1). In contrast, Pb, a common substitution for Bi in both bohdanowiczite and matildite (Table 1), was not recorded in the sample from Photo Lake. The Se substitutions are S (an average 8.38 wt.%) and traces of Te (0.02 wt.%; Table 1).

On the basis of these electron microprobe analytical data, and calculated for 4 ions, the average structural formula for this phase can be written as $[Bi_{0.925}Fe_{0.182}Sb_{0.011}]_{\Sigma 1.118}[Ag_{0.880}Cu_{0.094}]_{\Sigma 0.974}[S_{1.049}Se_{0.870}]_{\Sigma 1.919}$ (Table 1).

Discussion

The extent of the Se–S substitution between bohdanowiczite and matildite

The cation substitutions within bohdanowiczite and matildite, revealed by the literature compilation (Table 1) are relatively limited: the sum of substitution element concentrations does not exceed 2 wt.% in the vast majority of compositions reported (Table 1; Fig. 3). Therefore, there is no need to examine and re-evaluate our knowledge of these minerals from the point of view of cation substitutions, as they are limited and relatively well understood (e.g. Förster *et al.*, 2005, Vikentieva *et al.*, 2008, Cabral *et al.*, 2017).

The situation with the anion site is the exact opposite: the new data for the mineral from the Photo Lake deposit (Canada), reported here, show a very significant S replacement of Se (Fig. 4), significantly more than reported previously (Banas *et al.*, 1980; Sejkora and Skacha, 2015) thus prompting the question about a possible matildite–bohdanowiczite solid solution.

A substantial S replacement of Se in bohdanowiczite was reported recently at the Moldava fluorite deposit (Krušné hory Mountains, Czech Republic), in which S varies between 0.54 and 0.79 apfu (Fig. 4), which suggested to the authors the

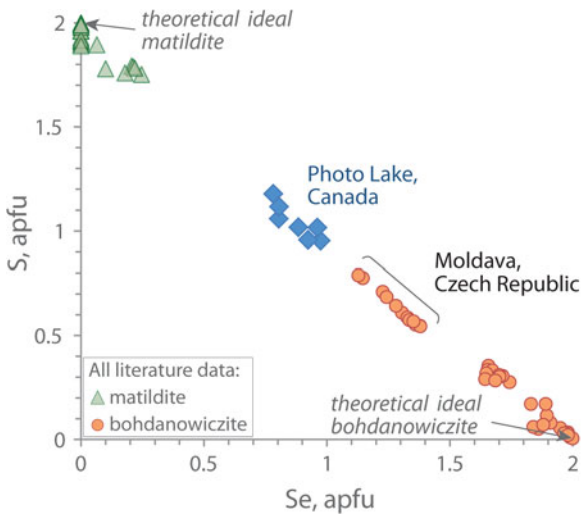

Fig. 4. The main anion substitution in the matildite–bohdanowiczite space, Se–S, based on the literature data in Table 1. Tellurium is always relatively low, at 0.03 apfu on average (Table 1). The samples from the Moldava (Sejkora and Skacha, 2015) and Photo Lake (this work) deposits clearly indicate that a complete solid solution may exist, as suggested previously by Banas *et al.* (1980) and Sejkora and Skacha (2015).

possibility of matildite–bohdanowiczite isomorphism (Sejkora and Skacha, 2015). The S substitution in bohdanowiczite from Kletno (Poland) averages at 0.17 apfu, was also interpreted to indicate the possibility of a matildite–bohdanowiczite solid solution (Banas *et al.*, 1980).

The Photo Lake matildite–bohdanowiczite mineral is sulfur-dominated, with S varying from 0.953 to 1.178 apfu (1.052 apfu on average) and Se from 0.782 to 0.975 apfu (0.858 apfu on average; Table 1, Fig. 4). Importantly, these new data from Photo Lake, combined with all available data for bohdanowiczite, cover the Se–S replacement range completely between Se_2S_0 to $Se_{0.78}S_{1.18}$; it is also entirely covered from $Se_{0.25}S_{1.75}$ to Se_0S_2, corresponding to the full matildite range (Fig. 4). Hence, the only portion of the full bohdanowiczite–matildite Se–S substitution range that is not known to exist is between $Se_{0.78}S_{1.18}$ to $Se_{0.25}S_{1.75}$, or ~28% of the full Se–S range (Fig. 4). These observations suggest that the matildite–bohdanowiczite solid solution might indeed exist, regardless of the limited number of reliable data reported here. Both end-member minerals belong to the same trigonal crystal system (hexagonal scalenohedral class, $\bar{3}2/m$), also endorsing the possibility of a complete solid solution.

Matildite–bohdanowiczite solid solution or a new mineral species?

Given that the full S–Se replacement range between matildite and bohdanowiczite has not been documented, either in the literature data, or with the with the new data from the Photo Lake mineral (Fig. 4), it may be argued that the data reported here (Table 1) do not correspond to a full matildite–bohdanowiczite solid-solution series, but rather to a series of distinct mineral species. The data approximately in the middle of the Se–S compositional range (Fig. 4), corresponding to the Moldava and Photo Lake samples, would have an empirical structural formula $Bi_{0.991}Ag_{0.999}Fe_{0.173}Cu_{0.030}Sb_{0.011}Pb_{0.008}Se_{1.162}S_{0.755}$, corresponding to a mineral compositionally defined as $BiAgSe_xS_{2-x}$ ($x = 0.78$ to 1.4).

In favour of this idea could be the slightly different amounts of major cations in the three minerals: on average matildite contains 52.94 wt.% Bi and 27.02 wt.% Ag, the Photo Lake mineral contains 48.43 wt.% Bi and 23.50 wt.% Ag, and bohdanowiczite contains 44.74 wt.% Bi and 22.49 wt.% Ag, (Table 1). This regular variation is however due to the need to balance the changing charges during the varying S–Se substitutions ($Se_{0.05}S_{1.92}$ in matildite, $Se_{1.72}S_{0.30}$ in bohdanowiczite, and $Se_{0.86}S_{1.05}$ in the Photo Lake sample: Table 1) and is not, in reality, an argument to suggest the existence of a new mineral species.

Another argument could be the existence of several distinct mineral species in the bismuthinite (Bi_2S_3) to guanajuatite (Bi_2Se_3) continuum (e.g. laitakarite $Bi_4(Se,S)_3$ and ikunolite $Bi_4(S,Se)_3$), covering the full range of S–Se substitutions (Prsek and Peterec 2008, Cook *et al.*, 2021; Fig. 1). One of the reasons behind defining discrete mineral species here is their distinct crystalline structures: bismuthinite and guanajuatite are orthorhombic whereas laitakarite and ikunolite are hexagonal (Anthony *et al.*, 1990). Both matildite and bohdanowiczite have the same crystalline structure ($\bar{3}2/m$), which is consistent with the existence a complete solid-solution series, analogous to the galena–clausthalite solid-solution series, where both end-member minerals have cubic structures.

In light of these comments, we suggest that the likelihood of new mineral species, occupying approximately the middle of the S–Se substitution range between matildite and bohdanowiczite, is rather low. The alternative explanation for the new and historical compositional data (Fig. 4) is the existence of a complete solid-solution series between matildite and bohdanowiczite. This conclusion is somewhat weakened by three factors: the lack of compositional data between $Se_{0.78}S_{1.18}$ and $Se_{0.25}S_{1.75}$, or approximately a quarter of the S–Se substitution range; the lack of crystallinity information for the matildite–bohdanowiczite sample from Photo Lake; and the relatively low number ($n = 7$) of new analyses. Regardless of these limitations, the possibility of the existence of a full solid-solution series between matildite and bohdanowiczite is high.

Matildite–bohdanowiczite solid solution and deposit formation

A review of the matildite and bohdanowiczite paragenesis reveals that they are present in a variety of deposit types. For example: orogenic gold deposits (Vikenteva *et al.*, 2008); high-sulfidation epithermal deposits (Triantafyllidis, 2019); polymetallic vein-type deposits (Shizimu *et al.*, 1998; Staude *et al.*, 2010); porphyry-related deposits (Auge *et al.*, 2005; Prsek and Peterec, 2008); VMS deposits (Belogub *et al.*, 2020; this work); and polymetallic or U vein deposits (Cabral *et al.*, 2017; Förster, 2005). Regardless of this variability in deposit type, the common factor is that they form at moderate to high temperatures.

This observation is consistent with the peak temperatures of ~350°C conditions prevailing in the Snow Lake area, host of the Photo Lake deposit. However, bohdanowiczite forms at relatively low temperatures, typically <120°C (Cabral *et al.*, 2017) and matildite at temperatures below ~200°C (Vikenteva *et al.*, 2008). To reconcile the contradiction between the high-temperature nature of the deposits where matildite and bohdanowiczite have been found, and the relatively low formation temperatures for both minerals, we suggest their formation during later post-peak temperature stages. This is certainly the case at Photo Lake, where the matildite–bohdanowiczite formed during a late stage following the main ore stage (Aisida, 2023). Simplistically, the formation of the matildite–bohdanowiczite in the approximately middle of the S–Se substitution composition, and the end-members matildite and bohdanowiczite, could involve main ore formation at relatively high temperatures, followed by a discrete low-temperature stage during which the relevant elements – Bi, Ag, S and Se – would be exsolved from the main ore minerals, as seems to be the case at Photo Lake.

It is also tempting to connect the presence of the mineral in the matildite–bohdanowiczite solid solution, or of its end-members, with a particular VMS deposit group. However, the VMS deposits in the Snow Lake area, which all belong to the same group and formed under the same conditions, have a very significant trace-mineral variability (Alexandre *et al.*, 2019; Aisida 2023). For instance, of three deposits situated in close vicinity, Chisel Lake is Ag and Sb rich (Alexandre *et al.*, 2019), Osborne Lake is Mo and Co rich, and Photo Lake is the only one in the area with a significant Bi mineral paragenesis (native bismuth, bismuthinite and matildite–bohdanowiczite; Aisida 2023). Indeed, it would seem that at least the Snow Lake VMS deposits have a reproducible main ore mineralogy (chalcopyrite, sphalerite, and galena, albeit in varying proportions), though have a very significant variability in accessory minerals (Aisida *et al.*, 2023), and that the presence of matildite–bohdanowiczite or its end-members would be dependent on a complex set of factors that are beyond the scope of this contribution.

Summary

The new, albeit very few compositional data for a Bi–Ag S–Se mineral observed in the Photo Lake VMS deposit (Manitoba, Canada), combined with a complete literature compilation of matildite and bohdanowiczite compositional data (Table 1), reveals a nearly complete range of S–Se substitution, with only the section between $Se_{0.78}S_{1.18}$ and $Se_{0.25}S_{1.75}$ not currently documented (Fig. 4). At the very least, these observations demonstrate a very wide range of S–Se substitution between matildite and bohdanowiczite, suggesting that a complete solid solution might indeed exist, as suspected already (Banas *et al*., 1980; Sejkora and Skacha, 2015), and analogous to the galena–clausthalite complete solid-solution series (Coleman 1959; Förster 2005; Fig. 1). The presence of a new mineral species half-way between matildite and bohdanowiczite is considered unlikely.

Acknowledgements. The authors are thankful to A. Baig (Brandon University) and P. Yang (University of Manitoba) for their generous help with SEM and EMPA, respectively. This project received no funding. Two anonymous reviewers, the Associate Editor Dr. David Good, and the Principal Editor Dr. Roger Mitchell are thanked for providing specific, thorough, and helpful comments and editorial guidance and assistance, resulting in a significantly improved manuscript.

Competing interests. The authors declare none.

References

Aisida M. (2023) *Ore Mineral Chemistry of the Snow Lake VMS Deposits*. MSc thesis at Brandon University, Canada.

Alexandre P., Heine T., Fayek M., Potter E. and Sharpe R. (2019) Ore mineralogy of the Chisel Lake Zn–Cu–Ag (+Au) VMS deposit in the Flin Flon-Snow Lake Domain, Manitoba, Canada. *The Canadian Mineralogist*, **57**, 925–945.

Anthony J.W., Bideaux R.A., Bladh K.W. and Nichols M.C. (1990) *Handbook of Mineralogy: Volume I; Elements, Sulfides, Sulfosalts*. Mineral Data Publishing, Tucson, Arizona, USA, 588 pp.

Auge T, Petrunov R and Bailly L (2005) On the origin of the PGE mineralization in the Elatsite porphyry Cu-Au deposit, Bulgaria: comparison with the Baula-Nuasahi complex, India, and other alkaline PGE-rich porphyries. *The Canadian Mineralogist*, **43**, 1355–1372.

Banas M. and Ottemann J. (1967) Bohdanowiczyt-nowy naturalny selenek srebra i bizmutu z Kletna w Sudetach (A new natural silver and bismuth selenide from Kletno in the Sudetes Mts). *Przeglad Geologiczny*, **5**, 240 [in Polish].

Banas M., Atkin D., Bowles J.F.W. and Simpson P.R. (1979) Definitive data on bohdanowiczite, a new silver bismuth selenide. *Mineralogical Magazine*, **43**, 131–133.

Banas M., Atkin D., Bowles J.F.W. and Simpson P.R. (1980) Further studies of Bohdanowiczite ($AgBiSe_2$) and some associated minerals. *Bulletin de Mineralogie*, **103**, 107–112.

Barton Jr. P.B. and Bethke PM (1987) Chalcopyrite disease in sphalerite: pathology and epidemiology. *American Mineralogist*, **72**, 451–467.

Belogub E.V., Ayupova N.R., Krivovichev V.G., Novoselov K.A., Blinov I.A. and Charykova M.V. (2020) Se minerals in the continental and submarine oxidation zones of the South Urals volcanogenic-hosted massive sulfide deposits: A review. *Ore Geology Reviews*, **122**, 103500.

Bondarenko S., Grinchenko O. and Semka V. (2005) Au–Ag–Te–Se mineralization in the Potashnya gold deposit, Kocherov tectonic zone, Ukrainian Shield. *Geochemistry, Mineralogy, and Petrology*, **43**, 20–25.

Cabral A.R., Ließmann W., Jian W. and Lehmann B. (2017) Bismuth selenides from St. Andreasberg, Germany: an oxidised five-element style of mineralisation and its relation to post-Variscan vein-type deposits of central Europe. *International Journal of Earth Sciences (Geologische Rundschau)*, **106**, 2359–2369.

Coleman R.G. (1959) The natural occurrence of galena – clausthalite solid solution. *American Mineralogy*, **44**, 166–174.

Cook N.J. and Ciobanu C.L. (2001) Paragenesis of Cu–Fe ores from Ocna de Fier-Dognecea (Romania), typifying fluid plume mineralization in a proximal skarn setting. *Mineralogical Magazine*, **65**, 351–372.

Cook N.J., Ciobanu C.L., Slattery A.D., Wade B.P. and Ehrig K. (2021) The mixed-layer structures of ikunolite, laitakarite, joséite-B and joséite-A. *Minerals*, **11**, 920.

Förster H.-J. (2005) Mineralogy of the U–Se-polymetallic deposit Niederschlema–Alberoda, Erzgebirge, Germany. IV. The continuous clausthalite–galena solid-solution series. *Neues Jahrbuch für Mineralogie - Abhandlungen*, **181**/2, 125–134.

Förster H.-J., Tischendorf G. and Rhede D. (2005) Mineralogy of the Niederschlema-Alberoda U–Se polymetallic deposit, Erzgebirge, Germany. V. Watkinsonite, nevskite, bohdanowiczite and other bismuth minerals. *The Canadian Mineralogist*, **43**, 899–908.

Govindarao B., Pruseth K.L. and Mishra B. (2018) Sulfide partial melting and chalcopyrite disease: an experimental study. *American Mineralogist*, **103**, 1200–1207.

Harris D.C. and Thorpe R.I. (1969) New observations on matildite. *The Canadian Mineralogist*, **9**, 655–662.

Ivashchenko V.I. (2021) Rare-metal (In, Bi, Te, Se, Be) mineralization of skarn ores in the Pitkäranta Mining District, Ladoga Karelia, Russia. *Minerals*, **11**, 124.

Kovalenker V.A. and Plotinskaya O.Y. (2005) Te and Se mineralogy of Ozernovskoe and Prasolovskoe epithermal gold deposits, Kuril – Kamchatka volcanic belt. *Geochemistry, Mineralogy, and Petrology*, **43**, 118–123.

Kullerud K., Kotková J., Šrein V., Drábek M. and Škoda R. (2018) Solid solutions in the system acanthite (Ag_2S)–naumannite (Ag_2Se) and the relationships between Ag-sulfoselenides and Sebearing polybasite from the Kongsberg silver district, Norway, with implications for sulfur–selenium fractionation. *Contributions to Mineralogy and Petrology*, **173**, 71.

Kuznetsov S.K., Sokerina N.V., Filippov V.N., Sorekin M.Y. and Zharkov V.A. (2012) Selenium minerals in gold bearing veins of the North Urals. *Doklady Akademii Nauk*, **442**, 390–393.

Lowry D. (1993) First occurrences of matildite ($AgBiS_2$) associated with Caledonian intrusives in Scotland. *Mineralogical Magazine*, **57**, 751–755.

Nesterov Y.G., Begizov V.D., Zavyalov Y.N., Kryukov V. and Chvileva T.N. (1985) First discovery of bohdanowiczite in USSR. *Zapiski Rossiiskogo Mineralogicheskogo Obshchestva*, **114**, 212–216 [in Russian].

Palache C., Berman H. and Frondel C. (1944) *The System of Mineralogy of James Dwight Dana and Edward Salisbury Dana Yale University 1837–1892, Volume I: Elements, Sulfides, Sulfosalts, Oxides*. John Wiley and Sons, Inc., New York. 7th edition, revised and enlarged [pages 429–430].

Pehrsson S., Gibson H.L. and Gilmore K. (2016) A special issue on volcanogenic massive sulfide deposits of the Trans-Hudson orogen: preface. *Economic Geology*, **111**, 803–816.

Pouchou J.L. and Pichoir F. (1984) *La Recherche Aerospatiale*, **5**, 349–367.

Pouchou J.L. and Pichoir F. (1985) "PAP" (φρZ) procedure for improved quantitative microanalysis. Pp. 104–106 in: *Microbeam Analysis* (J.T. Armstrong, editor). San Francisco Press, San Francisco.

Pring A. (1988) Selenides and sulphides from Iron Monarch, South Australia. *Neues Jahrbuch für Mineralogie - Abhandlungen*, **36**, 48.

Pringle G.J. and Thorpe R.I. (1980) Bohdanowiczite, Junoite and laitakarite from the Kidd Creek mine, Timmins, Ontario. *The Canadian Mineralogist*, **18**, 353–360.

Prsek J. and Peterec D. (2008) Bi–Se–Te mineralization from Úhorná (Spišsko Gemerské Rudohorie Mts., Slovakia): A preliminary report. *Mineralogia, Mineralogical Society of Poland*, **39**, 87–103.

Satory S., Ogata T. and Watanabe Y. (2017) Bismuth and tellurium minerals from the Arakawa Deposit in the Northeast Japan Arc. *International Journal of the Society of Materials Engineering*, **23**, 178–183.

Schonwandt H.K. (1983) Interpretation of microstructures from a selenous Cu-mineralization in South Greenland. *Neues Jahrbuch Mineralogie*, **146**, 203–332.

Sejkora J. and Skacha P. (2015) Selenidy z fluoritového ložiska Moldava v Krušných horách (Česká republika) (Selenides from the fluorite deposit

Moldava, Krušné hory Mountains (Czech Republic)). *Bulletin of Mineralogy and Petrology*, **23**, 229–241 [in Czech].

Sejkora J., Srein V., Sreinova B. and Dolnicek Z. (2017) Selenidová mineralizace uranového ložiska Potůčky v Krušných horách (Česká republika) (Selenide mineralization of the uranium deposit Potůčky, Krušné hory Mountains (Czech Republic)). *Bulletin of Mineralogy and Petrology*, **25**, 306–317 [in Czech].

Shizimu M., Kato A. and Matsuyama F. (1998) Two Se-bearing Ag–Bi sulphosalts, benjaminite and matildite from the Ikuno Deposits, Hyogo Prefecture, Japan – Au–Ag mineralization in polymetallic zone. *Resource Geology*, **48**, 117–124.

Staude S, Dorn A, Pfaff K and Markl G (2010) Assemblages of Ag-Bi sulfosalts and conditions of their formation: the type locality of schapbachite ($Ag_{0.4}Pb_{0.2}Bi_{0.4}S$) and neighboring mines in the Schwarzwald ore district, southern Germany. *The Canadian Mineralogist*, **48**, 441–466.

Stern R.A., Syme E.C., Bailes A.H. and Lucas S.B. (1995) Paleoproterozoic (1.90–1.86 Ga) arc volcanism in the Flin Flon Belt, Trans-Hudson Orogen, Canada. *Contributions to Mineralogy and Petrology*, **119**, 117–141.

Thorpe R.I., Pringle G.J. and Plant A.G. (1976) Occurrence of selenide and sulphide minerals in bornite ore of the Kidd Creek massive sulphide deposit, Timmins, Ontario. *Geological Survey of Canada Paper*, **76–1A**, 311–317.

Triantafyllidis S. (2019) Precious and critical metal phases in the Agios Filippos high-sulfidation epithermal system, Kirki, Thrace, NE Greece. *15th International Congress of the Geological Society of Greece, Athens*, 22–24 *May*, 2019.

Vikenteva O.V., Sergeeva N.E. and Eremin N.I. (2008) Finding of matildite in veins of the Berezovsk Gold Deposit, Ural Mountains. *Doklady Earth Sciences*, **418**, 5–8.

Zavyalov Y.N. (1985) Isostructural characteristics of bohdanowiczite and volynskite. *Zapiski Rossiiskogo Mineralogicheskogo Obshchestva*, **114**, 434–440 [in Russian].